Intersensor Calibration Between F13 SSMI and F17 SSMIS for Global Sea Ice Data Records

Donald J. Cavalieri, Claire L. Parkinson, Nicolo DiGirolamo, and Alvaro Ivanoff

***Abstract*—An intercalibration between F13 Special Sensor Microwave Imager (SSMI) and F17 Special Sensor Microwave Imager Sounder (SSMIS) sea ice extents and areas for a full year of overlap is undertaken preparatory to extending the 1979–2007 National Aeronautics and Space Administration (NASA) Goddard Space Flight Center NASA Team algorithm time series of global sea ice extents and areas. The 1979–2007 time series was created from Scanning Multichannel Microwave Radiometer (SMMR) and SSMI data. After intercalibration, the yearly mean F17 and F13 difference in northern hemisphere (NH) sea ice extents is -0.0156%, with a standard deviation (SD) of the differences of 0.6204%, and the yearly mean difference in NH sea ice areas is 0.5433%, with an SD of 0.3519%. For the southern hemisphere, the yearly mean difference in sea ice extents is $0.0304\% \pm 0.4880\%$, and the mean difference in sea ice areas is $0.1550\% \pm 0.3753\%$. This F13/F17 intercalibration enables the extension of the 29-year 1979–2007 SMMR/SSMI sea ice time series for as long as there are stable F17 SSMIS brightness temperatures available.**

***Index Terms*—Climate data records, sea ice, microwave remote sensing.**

I. Introduction

EARTH-OBSERVING satellites have proven to be extremely valuable for monitoring our changing planet [1] and for serving as the basis of producing long-term geophysical data records [2]. The utility of these long-term data records depends on the generation of a consistent set of measurements made from different sensors on different satellites over many years. One of the longest such data records is that for sea ice, which spans 30+ years and is distributed by the National Snow and Ice Data Center (NSIDC) [3]. The approach followed in the generation of the National Aeronautics and Space Administration (NASA) Goddard Space Flight Center (GSFC) NASA Team (NT) algorithm sea ice data record was to match the various data sets at the sea ice product level rather than at the satellite radiance level [4]. This approach has also been followed by the majority of end users in the generation of long-term time series of geophysical variables, for example, snow water equivalent [5]. The rationale for this approach stems from the complications that arise when trying to match brightness temperatures for scenes partially covered with water and has been discussed in detail in [6].

The existing intercalibrated NASA GSFC sea ice data record spans the period from October 26, 1978, through December 31, 2007, and is based on data obtained from the NASA Nimbus 7 Scanning Multichannel Microwave Radiometer (SMMR) (October 26, 1978, through August 20, 1987), the Defense Meteorological Satellite Program (DMSP) F8 Special Sensor Microwave Imager (SSMI) (July 9, 1987, through December 18, 1991), the DMSP F11 SSMI (December 3, 1991, through January 12, 1998), and the DMSP F13 SSMI (May 3, 1995, through December 31, 2007). The DMSP F13 SSMI started to degrade in 2008. A new sensor called the Special Sensor Microwave Imager Sounder (SSMIS) combined the SSMI conically scanning capability with high-frequency sounding channels and was first launched on the DMSP F16 satellite in 2003 [7], with a second SSMIS launched in 2006 on DMSP F17. The SSMIS on the DMSP F17 satellite has an ascending node crossing time closer to the DMSP F13 SSMI than the F16 SSMIS, and hence, the F17 SSMIS was selected to extend the sea ice time series through deliberations among W. Meier of the NSIDC and D. Cavalieri and C. Parkinson of NASA GSFC. The F17 SSMIS data extend from December 14, 2006, to the present, and we use the full year 2007 of data overlap with the F13 SSMI to intercalibrate the sea ice time series from the F13 SSMI and the F17 SSMIS.

The source of the calibrated F17 SSMIS brightness temperature data is Remote Sensing Systems, Inc. These brightness temperature data are gridded and distributed by NSIDC [8].

II. Procedure for Matching F13 and F17 Sea Ice Extents and Areas

The following procedure used daily SSMI polar stereographic grids with both a land mask and a sea surface temperature mask applied as described in [4]. We also filtered out those days with no data or days with missing orbits (32 days out of 365) before undertaking the following steps.

First, F13 and F17 brightness temperature (TB) histograms for both hemispheres and for each channel used in the NT sea ice concentration algorithm (19H, 19V, 22V, and 37V, standing for 19-GHz horizontally polarized data, 19-GHz vertically polarized data, etc.) were generated for the entire year of overlap (Fig. 1). The histograms show that the minimum TB's are nearly identical for F13 and F17 for all channels except 37V, where the F17 TB's are slightly greater than those for F13. For each channel, we added approximately 5% of the full range

Manuscript received July 5, 2011; revised August 2, 2011; accepted August 17, 2011. This work was supported by the Cryosphere Program at the National Aeronautics and Space Administration Headquarters.

D. J. Cavalieri is with D J Cavalieri Consulting, Sandy Spring, MD 20860 USA and also with the NASA Cryospheric Sciences Laboratory, Goddard Space Flight Center, Greenbelt, MD 20771 USA.

C. L. Parkinson is with the NASA Cryospheric Sciences Laboratory, Goddard Space Flight Center, Greenbelt, MD 20771 USA.

N. DiGirolamo is with the Science Systems and Applications, Inc., Lanham, MD 20706 USA and also with the NASA Cryospheric Sciences Laboratory, Goddard Space Flight Center, Greenbelt, MD 20771 USA.

A. Ivanoff is with the ADNET Systems, Inc., Rockville, MD 20852 USA and also with the NASA Cryospheric Sciences Laboratory, Goddard Space Flight Center, Greenbelt, MD 20771 USA.

Digital Object Identifier 10.1109/LGRS.2011.2166754

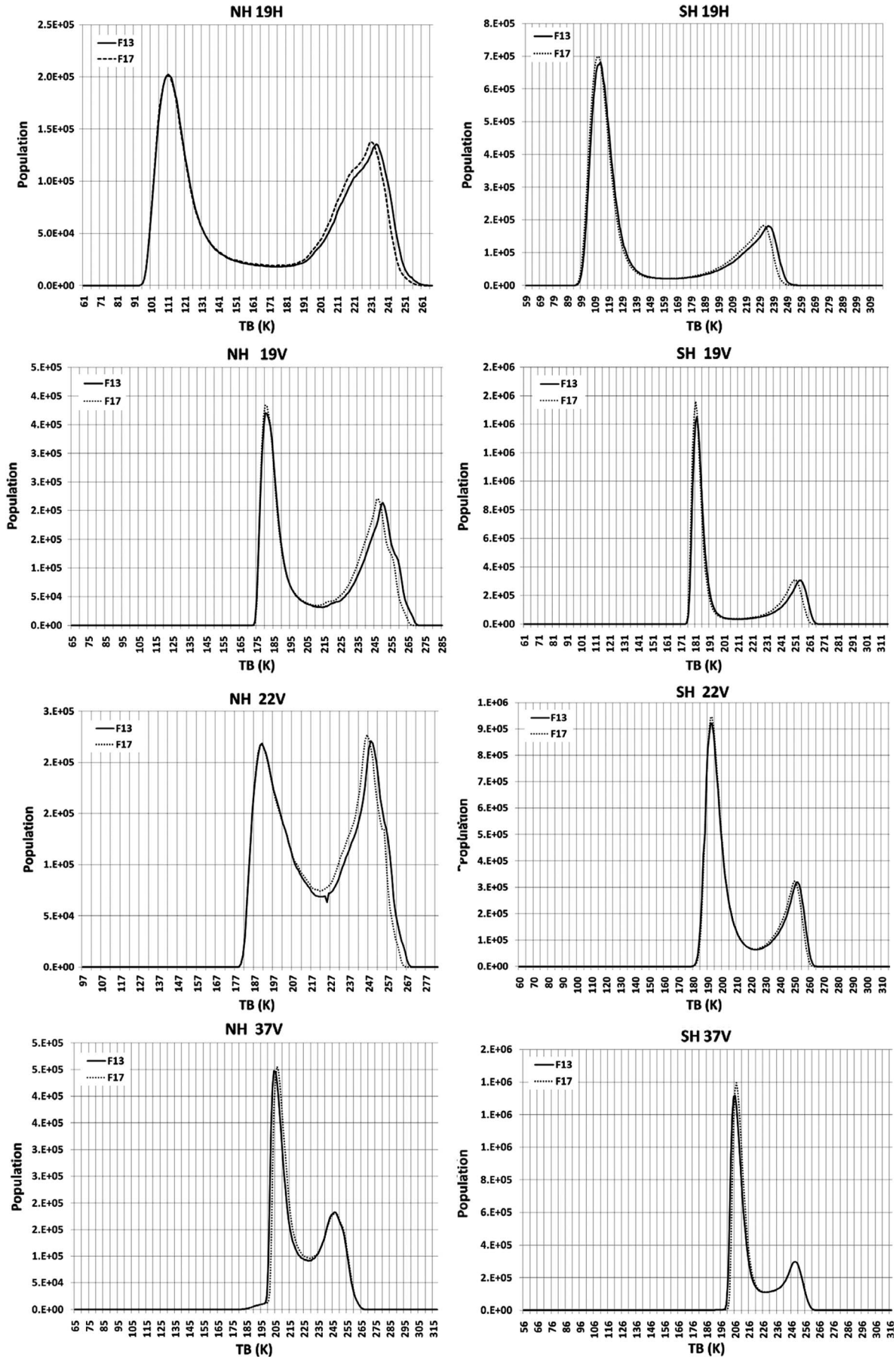

Fig. 1. F13 SSMI and F17 SSMIS TB histograms for each channel for the NH and SH.

TABLE I
F13 AND F17 TPS FOR OW, NH FIRST-YEAR ICE (FYI) AND MULTIYEAR ICE (MYI), AND SH ICE TYPE A AND ICE TYPE B. ICE TYPE A HAS SIMILAR MICROWAVE CHARACTERISTICS TO FYI IN THE NH, BUT ICE TYPE B IS A DIFFERENT ICE TYPE THAN MYI, POSSIBLY FYI WITH A HEAVY SNOW COVER; SEE [10] FOR FURTHER DETAILS. THE F13 TPS ARE FROM [4], WHILE THE F17 TPS ARE NEWLY CALCULATED AS DESCRIBED IN THIS LETTER

Northern Hemisphere	F13 TP (K)	F17 TP (K)	Southern Hemisphere	F13 TP (K)	F17 TP (K)
19V OW	185.2	184.9	19V OW	186.0	184.9
19H OW	114.4	113.4	19H OW	117.0	113.4
37V OW	205.2	207.1	37V OW	206.9	207.1
19V FYI	251.2	248.4	19V Ice Type A	256.0	253.1
19H FYI	235.4	232.0	19H Ice Type A	241.4	237.8
37V FYI	241.1	242.3	37V Ice Type A	245.6	246.6
19V MYI	222.4	220.7	19V Ice Type B	246.6	244.0
19H MYI	198.6	196.0	19H Ice Type B	214.9	211.9
37V MYI	186.2	188.5	37V Ice Type B	211.1	212.6

of TB's to the minimum TB to obtain a range of open water (OW) "minimum" TB's. For the high TB or sea ice end of the histogram, we subtracted approximately 10% of the range of TB's from the maximum TB to obtain a range of sea ice "maximum" TB's. Interestingly, all of the channels of F13 exhibit a slightly greater maximum TB than those of F17, except for the 37V channel, which shows almost identical maximum TB's (Fig. 1). Next, we filtered each TB map, keeping only the TB's in the minimum and maximum ranges, and then obtained linear regression coefficients (slope and intercept) between the F13 and F17 TB's for each day and channel.

Keeping only those regression coefficients within one standard deviation (SD), we calculated the yearly mean slopes and intercepts for each channel. Based on these mean slopes and intercepts, we computed the F17 sea ice algorithm tiepoints (TPs) for each hemisphere using the F13 TPs as input. Finally, for the southern hemisphere (SH), we used the northern hemisphere (NH) OW TPs, because they were slightly lower, and we also used a different weather threshold for the F17 algorithm. The two weather filters used in the NT algorithm are based on the following spectral gradient ratios:

$$GR(37/19) = [TB(37\text{V}) - TB(19\text{V})]/[TB(37\text{V}) + TB(19\text{V})]$$

$$GR(22/19) = [TB(22\text{V}) - TB(19\text{V})]/[TB(22\text{V}) + TB(19\text{V})].$$

Specifically, the thresholds used in the F17 SSMIS version of the NT sea ice algorithm are as follows.

1) If $GR(37/19) > 0.05$ for locations in the NH or > 0.053 for locations in the SH, then the ice concentration is set to zero.
2) If $GR(22/19) > 0.045$ for locations in either hemisphere, then the ice concentration is set to zero.

These weather filters and their effectiveness are discussed in detail in [9]. The only change to the threshold values given in [9] is the 0.053 threshold value for $GR(37/19)$ for the SH. No other adjustments were made. Both the F13 and the F17 TPs are presented in Table I.

III. RESULTS

Using the newly calculated F17 SSMIS TPs (Table I), Fig. 2 shows the plots of the daily percent difference between the F17 and F13 sea ice extents and areas for (a) the NH and (b) the SH. The figure also gives the annual mean and SD of the percent differences for each sea ice parameter and hemisphere. Scatter plots of F17-versus-F13 sea ice extents and areas for both hemispheres (not shown) give r-squared values of 0.9998 or higher.

The annual mean percent differences $\pm$ 1 SD between the F17 and F13 sea ice extents are $-0.0156\% \pm 0.6204\%$ and $0.0304\% \pm 0.4880\%$ for the NH and SH, respectively. Both of these mean percent differences are within the corresponding mean differences (0.05%) reported in [4] for the periods of sensor overlap in the 1978–1996 sea ice time series. For sea ice areas, the mean percent differences $\pm$ 1 SD are $0.5433\% \pm 0.3519\%$ and $0.1550\% \pm 0.3753\%$ for the NH and SH, respectively. These mean percent differences for sea ice area are within the mean sea ice area difference of 0.6% reported in [4] for the periods of sensor overlap in the 1978–1996 time series.

The largest excursions from the zero percent difference line for both the NH and SH sea ice extents occur during the summer months (Fig. 2), when there are larger temporal changes than during the winter months. The ascending node crossing times are different for F13 and F17, and this difference may be particularly important during summer, when there is greater ice-edge melt variability. The variations in sea ice area do not appear as large or as sudden as the variations in sea ice extent, which is more susceptible to day-to-day weather forcing. This is also reflected in the somewhat smaller sea ice area annual SDs.

IV. CONCLUSION

The DMSP F17 SSMIS NT sea ice concentration algorithm TPs derived in this study result in mean differences between the F13 SSMI and F17 SSMIS sea ice extents and areas of less than 0.031% and 0.6%, respectively, for both hemispheres for the year of overlap, 2007. These mean differences are similar to those obtained previously when matching earlier sensors on different satellites in the generation of the current NASA GSFC sea ice time series [4]. The earlier intersensor calibrations were limited by the relatively short periods of sensor overlap of good data. These overlap periods were 22 days for the Nimbus 7 SMMR/DMSP F8 SSMI, 16 days for the DMSP F8/F11 SSMIs, and 5 months for the DMSP F11/F13 SSMIs. These overlap periods are in sharp contrast to the full year of overlap used for the F13/F17 intersensor calibration presented here. The much longer period of overlap in this study could account for why the agreements between the F13 and F17 sea ice extents and areas are not substantially better than the agreements obtained with the earlier sensor overlap periods, as there is more possibility for intersensor variability over a full year than over shorter periods (for example, winter versus summer). Furthermore, the level of agreement obtained previously required subjective tuning of some of the TPs [4].

The DMSP F17 SSMI NT sea ice concentration algorithm TPs obtained in this study will allow us to extend the NASA GSFC sea ice time series into the future for as long as there are stable F17 SSMIS brightness temperatures available. Future sensors should be planned to ensure that there is at least one year of overlap between each pair of successive SSMIS sensors.

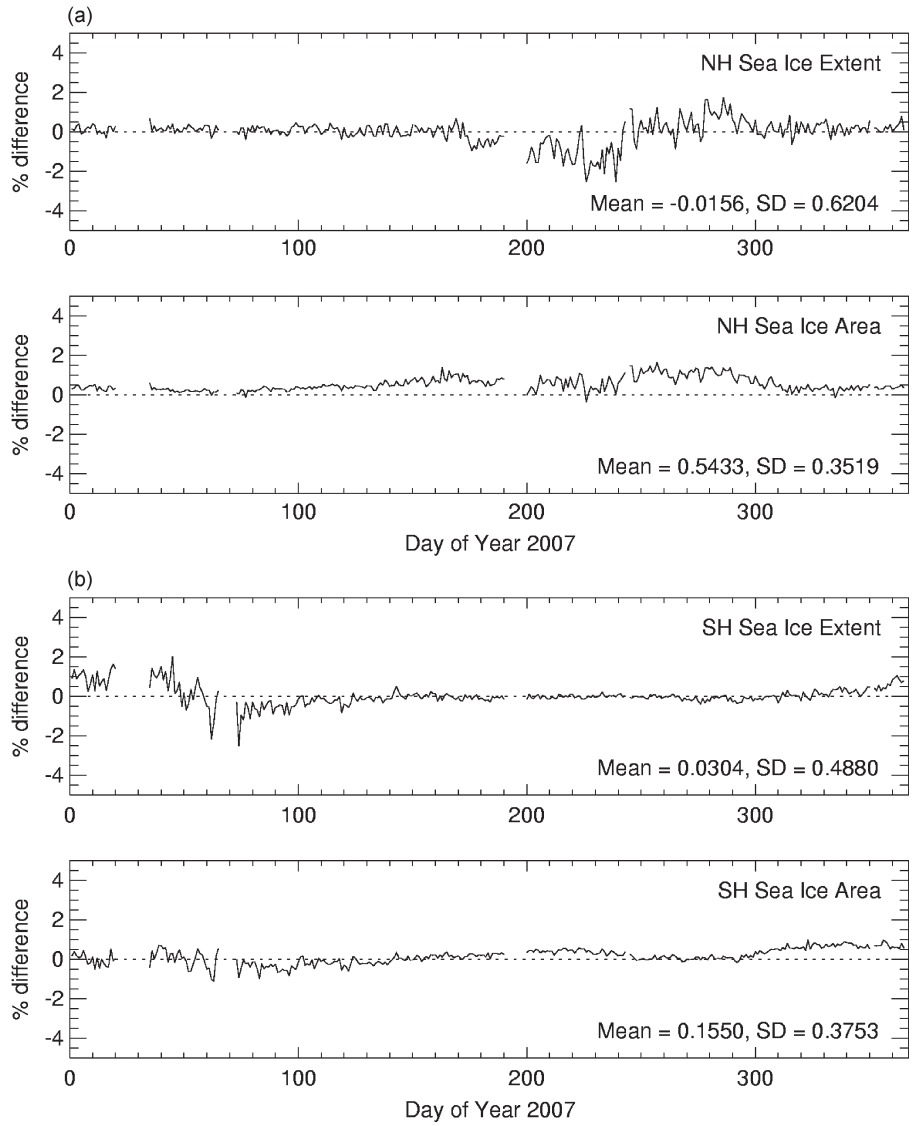

Fig. 2. Time series of the daily percent differences between F17 and F13 sea ice extents and areas for 2007 based on the newly derived F17 sea ice TPs (Table I) for (a) the NH and (b) the SH. Percent differences are calculated as $100 \cdot (F17 - F13)/F13$.

ACKNOWLEDGMENT

The authors would like to thank Dr. W. Meier of the National Snow and Ice Data Center (NSIDC), Boulder, CO, for discussions regarding the selection of the Defense Meteorological Satellite Program (DMSP) Special Sensor Microwave Imager Sounder (SSMIS) sensor to extend the time series. The authors acknowledge the receipt of the 2007 DMSP F17 SSMIS daily polar gridded brightness temperatures from the NSIDC.

REFERENCES

[1] M. D. King, C. L. Parkinson, K. C. Partington, and R. G. Williams, Eds., *Our Changing Planet: The View from Space*. Cambridge, U.K.: Cambridge Univ. Press, 2007, p. 391.

[2] R. J. Gurney, J. L. Foster, and C. L. Parkinson, Eds., *Atlas of Satellite Observations Related to Global Change*. Cambridge, U.K.: Cambridge Univ. Press, 1993, p. 470.

[3] D. J. Cavalieri, C. Parkinson, P. Gloersen, and H. J. Zwally, *Sea Ice Concentrations from Nimbus-7 SMMR and DMSP SSM/I Passive Microwave Data*. Boulder, CO: Nat. Snow Ice Data Center, 1996, Digital media, updated 2008.

[4] D. J. Cavalieri, C. L. Parkinson, P. Gloersen, J. C. Comiso, and H. J. Zwally, "Deriving long-term time series of sea ice cover from satellite passive-microwave multisensor data sets," *J. Geophys. Res.*, vol. 104, no. C7, pp. 15 803–15 814, 1999.

[5] C. Derksen, A. Walker, E. LeDrew, and B. Goodison, "Combining SMMR and SSM/I data for time series analysis of central North American snow water equivalent," *J. Hydrometeorol.*, vol. 4, no. 2, pp. 304–316, Apr. 2003, DOI: 10.1175/1525-7541.

[6] I. H. H. Zabel and K. C. Jezek, "Consistency in long-term observations of oceans and ice from space," *J. Geophys. Res.*, vol. 99, no. C5, pp. 10 109–10 120, 1994.

[7] D. B. Kunkee, G. A. Poe, D. J. Boucher, S. D. Swadley, Y. Hong, J. E. Wessel, and E. A. Uliana, "Design and evaluation of the first Special Sensor Microwave Imager/Sounder," *IEEE Trans. Geosci. Remote. Sens.*, vol. 46, no. 4, pp. 863–883, Apr. 2008.

[8] J. Maslanik and J. Stroeve, *DMSP SSM/I-SSMIS Daily Polar Gridded Brightness Temperatures*. Boulder, CO: Nat. Snow Ice Data Center, 1990, Digital media, updated 2010.

[9] D. J. Cavalieri, K. St. Germain, and C. T. Swift, "Reduction of weather effects in the calculation of sea ice concentration with the DMSP SSM/I," *J. Glaciol.*, vol. 41, no. 139, pp. 455–464, 1995.

[10] P. Gloersen, W. J. Campbell, D. J. Cavalieri, J. C. Comiso, C. L. Parkinson, and H. J. Zwally, *Arctic and Antarctic Sea Ice, 1978-1987: Satellite Passive Microwave Observations and Analysis*. Washington, DC: Nat. Aeronaut. Space Admin., 1992, p. 290, Special Publication 511.